JOURNAL OF GEOPHYSICAL RESEARCH, VOL. 104, NO. A12, PAGES 28,351–28,360, DECEMBER 1, 1999

Structure of the magnetospheric magnetic field during magnetic storms

L. A. Dremukhina and Y. I. Feldstein

Institute of Terrestrial Magnetism, Ionosphere and Radio Wave Propagation, Troitsk, Russia

I. I. Alexeev and V. V. Kalegaev

Institute of Nuclear Physics, Moscow State University, Moscow

M. E. Greenspan

Department of Physics, University of Maryland, College Park

Abstract. We report the results of a study of the contributions of the large-scale magnetospheric currents to the observed *Dst* variation. Ground-based magnetometer data during four magnetic storms (January 27-30, 1985; November 23-27, 1986; January 14-16, 1988; and May 6-8, 1988) were used to calculate *Dst*, and the paraboloid model of the magnetospheric magnetic field [*Alexeev et al.*, 1996] was used to determine the contribution of each magnetospheric current system. Input data for our model were the solar wind plasma parameters, the interplanetary magnetic field (IMF) B_Z, DMSP F6, F7, F8, and F9 satellite observations of precipitating auroral particles, and Active Magnetospheric Particle Tracer Explorers (AMPTE)/CCE satellite measurements of the total energy of the ring current ions with energy per charge between 1.5 and 300 keVq^{-1}. We found good agreement between observed and modeled magnetic fields during the main phase of the magnetic storms. Using the paraboloid model, we have determined the contributions to *Dst* of different magnetospheric current systems including the magnetopause current B_{CF}, the symmetric ring current B_R, and the geotail current B_T. Such separation shows that values of B_T and B_{CF} are comparable with the value of B_R during the main phase of the storms. During the recovery phase the effect of B_R predominates.

1. Introduction

The *Dst* variation of the geomagnetic field commonly is ascribed to the development of the ring current in the inner magnetosphere. However the ring current development alone cannot explain certain observations. First, the magnetopause's earthward shift during a magnetic storm cannot be caused by the ring current enhancement. Second, there are rapid ($\sim 1-3$ hours) *Dst* changes during the recovery phase, while the typical timescale for change-exchange loss of ring current ions (the main mechanism of losses) is $\sim$ 10 hours [*Kozyra*, 1989; *Kistler et al.*, 1989; *Fok et al.*, 1993].

In recent years some authors have developed the idea that the tail current system significantly influences the *Dst* index [*Alexeev et al.*, 1992, 1996; *Arykov and Maltsev*, 1993; *Maltsev et al.*, 1994]. Indeed, the conclusion made by *Campbell* [1973, p. 171] was that " the large magnetic disturbance shows characteristics more of a magnetospheric tail sheet current than a ring current", but the triangulated hypothetical current method used by Campbell is too rough for numerical estimations. To calculate the magnetic perturbation caused by the tail current system, it is necessary to know the current distribution in the plasma sheet and on the magnetopause exactly. Such information is unavailable at present. However, it is possible to estimate the tail current system's effect on the *Dst* index by using the value of the tail lobe magnetic flux [*Maltsev*, 1991; *Alexeev et al.*, 1992]. In this work we present the results of a detailed study of four geomagnetic storms based on the paraboloid model of the magnetospheric magnetic field [*Alexeev*, 1978; *Alexeev et al.*, 1996]. The paraboloid model allows us to separate relative contributions to the *Dst* index caused by various sources: the ring current, the current on the magnetopause, and the current system of the magnetospheric tail. It is important that the paraboloid model describes the time variations of these magnetospheric current systems, because each of them develops on its own timetable. Therefore the paraboloid model has been selected to analyze the four

Paper number 1999JA900261.
0148-0227/99/1999JA900261$09.00

events that occurred on November 23-27, 1986; January 27-30, 1985; January 14-16, 1988; and May 6-8, 1988.

2. Calculations

According to the paraboloid model, the total magnetic disturbance inside the magnetosphere at any point is presented as

$$B_M(t) = B(t) - B_D = B_{SD}(t) + B_T(t) + B_R(t) + B_{SR}(t). \quad (1)$$

Here $B_M(t)$ is the total magnetic disturbance, $B(t)$ is the total magnetic field intensity inside the magnetosphere as a function of the time t, B_D is the dipole field, B_R is the field of the ring current's symmetric component, B_T is the field of the magnetospheric tail current system, and $B_{CF} = B_{SR} + B_{SD}$ is the field of the magnetopause currents screening the ring current field and the dipole field. A screening term for the tail current is included in the calculated tail current system's field. In the paraboloid model, Chapman-Ferraro (CF) currents are calculated using the condition that the normal component of the total magnetic field (the sum of the dipole magnetic field and the magnetic field created by the CF currents) on the magnetopause is equal to zero. The magnetic perturbations due to the tail currents are determined by the tail lobe magnetic flux and magnetospheric geometric parameters. The tail currents close on the dayside magnetopause and the tail lobes. The magnetic field due to the closure currents is calculated from the condition that the component normal to the magnetospheric boundary of the summed magnetic field of the tail currents and their closure currents on the magnetopause equal to zero. In other words, the magnetic perturbation due to the tail currents is calculated by solving Laplace's equation for a potential with the boundary condition $\vec{B} \cdot \vec{n} = 0$, similarly for the CF currents. There is a spatial overlap between the dayside closure of the tail current and the CF currents.

The observed magnetic field disturbance $B_M(t)$ also includes the contributions of other current systems such as the Region 1 and 2 field-aligned currents and the partial ring current. The disturbances due to the field-aligned and ionospheric currents make noticeable contributions to the asymmetry of the magnetic H component at low latitudes. The fields of these currents must be taken into account if the longitudinal asymmetry of the magnetic field at low latitudes during magnetic storms is to be analyzed. However, model calculations of the disturbance fields caused by the Region 1 and 2 field-aligned currents show that averaged over magnetic local time (MLT), the H component of the disturbance field is close to zero [*Sun et al.*, 1984; *Dremukhina et al.*, 1990]. The magnetic disturbances due to the field-aligned and ionospheric closure currents of the partial ring current behave similarly [*Takahashi et al.*, 1991]. Because the *Dst* index is the symmetric part of the magnetic field disturbance, the contribution of the ionospheric and field-aligned currents to *Dst* does not exceed a few nanotesla. Therefore the contribution of those currents to *Dst* was not considered.

To calculate the magnetic field disturbance using the paraboloid model, it is necessary to set five time-dependent input parameters: the geomagnetic dipole tilt angle ϕ; the geocentric distance from the Earth to the subsolar point, R_1; the geocentric distance from the Earth to the earthward edge of the magnetospheric tail current sheet, R_2; the geotail lobe magnetic flux Φ_∞; and the intensity of the ring current perturbation field at the Earth's center, B_{RO}.

The geomagnetic dipole tilt angle is a known function of the UT [see, e.g., *Alexeev et al.*, 1996]. In order to obtain the other four model parameters for the cases studied, empirical data were used: when available, solar wind density and velocity (N and V) and the north-south interplanetary magnetic field (IMF) component B_Z, results of a calculation of the total energy carried by ring current ions based on Active Magnetospheric Particle Tracer Explorers (AMPTE)/CCE satellite data in the inner magnetosphere, and DMSP F7-F9 satellite observations giving the locations of different precipitating particle populations in the high-latitude auroral region.

The *Dst* variation in the course of four selected storms has been calculated using 1 min data from the seven low-latitude magnetometer stations listed in Table 1. Deviations of the magnetic field horizontal components ΔH and ΔD from the quiet level during each minute were calculated using magnetograms from the seven observatories. We used magnetic field values taken on one of the quietest days before each storm as the quiet level.

Table 1. The List of Observatories Used for Calculations of *Dst*

	Geographic Coordinates, deg		Geomagnetic Coordinates, deg	
Observatory	Latitude	Longitude	Latitude	Longitude
Sun Juan	18.1	293.8	29.9	8.2
Tenerife	28.5	343.7	19.8	61.4
Tbilisi	44.7	47.9	36.8	116.6
Lunping	25.0	121.2	17.6	192.0
Kakioka	36.2	140.2	28.3	210.8
Honolulu	21.3	202.0	21.8	268.7
Dell Rio	29.3	259.2	39.0	324.1

The quiet days were January 25, 1985; November 22, 1986; January 9, 1988; and May 1, 1988. The resulting 1-min values of ΔH and ΔD were transformed to geomagnetic components ΔX and ΔY by rotation of the coordinate systems. We calculated values of ΔX at the Earth's equator from the data from each observatory by dividing by $\cos\lambda$, where λ is the geomagnetic latitude of the observatory. The equatorial values of ΔX for all observatories were averaged to give the 1-min *Dst*. Then we found the 1-hour *Dst* by averaging over 60 1-min *Dst*.

AMPTE/CCE data were used to calculate the ring current ion energy W. We used measured fluxes of hydrogen, helium, nitrogen, and oxygen ions with energies per charge from 1.5 to 300 keVq^{-1} to compute a local ring current energy density. We then multiplied that energy density by the appropriate dipole L shell volume, and we summed the resulting energies over the range L = 2-7 to get W. Longitudinal symmetry of the ring current was assumed. The time required for CCE to cross the range L = 2-7 was $\sim$ 3 hours. During intervals when the satellite was outside the ring current, W was calculated by linear interpolation. The intervals were $\sim$ 1 hour at perigee and $\sim$ 9 hours at apogee.

To calculate the other input parameters of the paraboloid model, we have utilized DMSP F6, F7, F8, and F9 electron and ion spectra taken every second, covering particle energies from 30 to 20 eV. These spectra have been used to identify the precipitating plasma boundaries in high-latitude regions and to determine the colatitude of the polar cap boundary θ_{pc}. Only Northern Hemisphere observations were used. During $\sim$ 15 min the DMSP satellite orbit intersects the auroral boundary twice in two different MLT sectors.

Newell et al. [1996] and *Feldstein and Galperin* [1996] describe the physical principles for selection of appropriate boundaries. We assume that the border marked by the equatorward boundary of the cusp or open low-latitude boundary layer (LLBL) (on the dayside) and by the poleward boundary of the subvisual drizzle (on the nightside) is the polar cap boundary [*Newell et al.*, 1996; *Feldstein and Galperin*, 1996]. The boundary between discrete and diffuse auroral precipitations is assumed to mark the equatorward boundary of the auroral oval. That boundary maps along the magnetic field lines to the inner edge of the geotail plasma current sheet near midnight. Then, supposing that the polar cap is a circle, the angular displacement of the polar cap center from the geomagnetic pole along the midday-midnight meridian, d_{pc}, and the angular polar cap radius θ_{pc} were calculated by using the measured coordinates (corrected geomagnetic latitude λ and MLT) of two points corresponding to every intersection of the auroral boundary and the satellite orbit. After that it became possible to calculate the paraboloid model parameter tail lobe magnetic flux Φ_∞ as

$$\Phi_\infty = 2\pi B_E R_E^2 \sin^2\theta_{pc}, \tag{2}$$

where B_E is the dipole field at the Earth's equator and R_E is the Earth's radius. The tail lobe magnetic flux Φ_∞ is an important parameter of the paraboloid model because it determines the intensity of the magnetospheric tail current system.

Another parameter of the paraboloid model is the geocentric distance, R_2, to the earthward edge of the dawn-dusk directed plasma sheet current. This parameter together with the parameter R_1 completely defines the scale of the magnetospheric tail current system closing over the magnetopause. Like Φ_∞, the parameter R_2 was derived from DMSP satellite data. As described above, the angular radius of a circle for the boundary between discrete and diffuse precipitation, $\theta(b3a)$, and the angular displacement of this circle from the geomagnetic pole along the midday-midnight meridian, $d(b3a)$, were calculated using DMSP observations. According to *Newell et al.* [1996], *b3a* is the boundary between discrete and diffuse auroral plasma precipitation, corresponding to the stable trapping boundary of electrons with energy $E > 35$ keV. This boundary marks a change in the magnetic field line character on the nightside of the magnetosphere from quasi-dipolar to extended magnetotail. The change results from the presence of the magnetospheric tail current sheet, and the boundary *b3a* identifies the location of the tail current sheet's earthward edge. The midnight colatitude of the boundary of discrete precipitation is equal to

$$\theta_n = \theta(b3a) + d(b3a). \tag{3}$$

In order to obtain the geocentric distance R_2, the boundary θ_n was projected to the magnetospheric equatorial plane assuming that the magnetic field lines are quasi-dipolar. During magnetic storms the inner boundary of the tail current frequently is located at R_2 = 4-5 R_E near midnight. Direct comparison between model values R_2 and measured AMPTE/CCE locations of the plasma sheet's inner boundary in the equatorial plane gives discrepancies from 0.1 to 0.6 R_E. Thus

$$R_2 = 1/\sin^2\theta_n. \tag{4}$$

The distance from the Earth to the subsolar point on the magnetopause R_1 is the input parameter which determines the scale of the magnetosphere. *Mead* [1964] made the first significant computation of the dependence of the magnetopause position (R_1) on the solar wind pressure. We have calculated R_1 using solar wind plasma and IMF data when available. Initially, we calculated R_1 using both the formula given by *Roelof and Sibeck* [1993] and that given by *Shue et al.* [1997] for the dependence of R_1 on the dynamic pressure of the solar wind P_{SW} and the IMF B_Z. Both functional forms give similar results for small values of the IMF B_Z. However, the formula of Roelof and Sibeck is valid only when $P_{SW} < 8$ nPa and $B_Z < 7$ nT. For this reason, we have used the functional form of Shue et al., which is valid over a wider range of P_{SW} and B_Z IMF values:

$$R_1 = (11.4 + 0.013 \times B_Z)/P_{SW}^{1/6.6} \qquad B_Z < 0;$$

$$R_1 = (11.4 + 0.140 \times B_Z)/P_{SW}^{1/6.6} \qquad B_Z > 0. \tag{5}$$

During the storms studied, there were many time intervals when the solar wind data were missing. During such intervals we calculated R_1 by the following method: the empirical dependence of R_1 on Φ_∞ was obtained for the periods during the four storms when solar wind data were available. The data were divided into three groups corresponding to three different levels of geomagnetic disturbance, which were specified by R_2: strong disturbed conditions if $R_2 < 4.5\ R_E$, moderately disturbed conditions if $4.5\ R_E \le R_2 \le 7.0\ R_E$, and quiet conditions if $R_2 > 7.0\ R_E$. Assuming a linear relation between R_1 and Φ_∞, the following dependence was found:

$$\begin{aligned} R_1 &= 8.30 \qquad R_2 < 4.5\ R_E, \\ R_1 &= -0.49\Phi_\infty + 9.45 \qquad 4.5\ R_E \le R_2 \le 7.0\ R_E, \\ R_1 &= 10.0 \qquad R_2 > 7.0\ R_E, \end{aligned} \tag{6}$$

Here R_1 is in R_E, and Φ_∞ is in 10^8 Wb.

For periods when the solar wind data are available, values of parameter R_1 obtained on the basis of relations (5) or (6) were recalculated by requiring balance between the solar wind dynamic pressure and the paraboloid model magnetic pressure. These values of R_1^* were used as input parameters for subsequent calculations of the model magnetic variations on the Earth's surface. Figures 1b, 3b, 5b, and 7b show R_1^* and R_1 as well as other input parameters of the paraboloid model (R_1^* is plotted as a solid line, and R_1 is plotted as a dashed line). As one can see from figures 1b, 3b,5b, and 7b, the values of R_1 and R_1^* do not differ from each other significantly (differences are $O(0.1\ R_E)$). During periods with southward IMF ($B_Z \ll 0$), $R_1^* > R_1$, and, in contrast, $R_1^* < R_1$ during periods with $B_Z > 0$.

The last parameter that is necessary for input to the paraboloid model is the ring current intensity. We calculated this parameter from the total ring current ion energy measured by the AMPTE/CCE satellite during the intervals studied. The total ring current particle kinetic energy W is related to the magnetic field perturbation at the Earth's center by the Dessler-Parker-Sckopke relation:

$$B_{R0} = -(2/3)B_E W/W_M. \tag{7}$$

Here B_{R0} is the magnetic field caused by the ring current at the Earth's center, B_E is the dipolar field at the Earth's equator, $W_M = (1/3)B_E M$ is the dipolar field energy outside of the Earth (M is the dipolar magnetic moment), and W is the total energy of the ring current particles. Because of the high conductivity of the Earth's mantle and core, the contribution of the symmetric ring current to Dst is equal to $B_R = (3/2)B_{R0}$. Since $B_E = 3.2 \times 10^4$ nT and $W_M = 8 \times 10^{24}$ ergs, for ions with total energy $W = 10^{31}$ keV one finds B_R=-64 nT. Calculations of W are based, as a rule, on the measurements made inside a limited local time sector by only one satellite. Therefore it is supposed that the ring current did not depend on longitude. However, this supposition clearly is not accurate during the main phase of a magnetic storm, when the total particle energy distribution strongly depends on MLT.

We compare the model magnetic field $B_M(t)$ obtained from (1) with the Dst variation, which is calculated relative to the quiet magnetic field. Therefore we must subtract from $B_M(t)$ the magnetic fields produced by quiet time currents. This means that the correction, $(B_{SD}^q + B_{SR}^q + B_T^q + B_R^q)$, containing the contributions of all sources during the quiet periods is required. Let us evaluate this correction using the paraboloid model. It is well known that during quiet intervals the auroral oval equatorward boundary is located at $\lambda \approx 70°$ near midnight and at $\lambda \approx 80°$ near midday [*Feldstein and Starkov*, 1967]. This gives values of the parameters $R_2 \sim 8\ R_E$ and $\Phi_\infty \sim 0.5 \times 10^9$ Wb. Parameters R_1 and B_{R0} are assumed to be $\sim 10\ R_E$ and -15 nT (owing to the ring current energy W before a storm). Then the paraboloid model gives the following values of magnetic disturbances on the Earth's surface: $B_{SD}^q \approx 33$ nT, $B_{SR}^q \approx 0.4$ nT, $B_T^q \approx -15$ nT, and $B_R^q \approx -22$ nT. The total correction is equal to -3.6 nT. It was omitted when comparing $B_M(t)$ with Dst because it is small.

3. Results

We have shown that it is possible to calculate the time dependence of R_1, R_2, Φ_∞, and B_{R0} during magnetic storms then use them to calculate the time dependence of the model field at the Earth's equator, and compare it with the $|Dst|$ variation. In our study we analyzed four moderate magnetic storms with $Dst \approx 120 - 150$ nT during the main phase.

3.1. Magnetic storm of November 23-27, 1986

Figure 1 shows the solar wind data available to evaluate the input parameters of the model. This storm was studied by *Kalegaev et al.* [1998]. Figure 1a shows the solar wind data (IMF B_Z, density N, and velocity V) and the calculated dynamic pressure P_{SW} in the interval November 23-27, 1986. Figure 1b represents the paraboloid model parameters: R_1, obtained from (5) (dashed line) and R_1^*, obtained from the balance between dynamic and magnetic pressures (solid line). Two other parameters plotted in Figure 1b, $R_2(R_E)$ and $\Phi_\infty/10^8$(Wb), have been calculated from (2) and (4) using DMSP satellite data. During intervals when the solar wind data are absent, values of R_1 are reconstructed from (6). Colatitudes of the polar cap midnight boundary $\theta_0 = \theta_{pc} + d_{pc}$ obtained from empirical data are shown in the bottom plot of Figure 1b. As one can see from Figure 1, variations of the paraboloid model input parameters reflect the effect of solar wind parameter changes. The solar wind velocity did not change significantly during the considered interval. Its values were $\sim 400-500$ kms^{-1}. However, the density N and the IMF B_Z changed very significantly: N changed from 5 to 30 cm^{-3}, and B_Z changed from -10 to +15 nT. There are three intervals of increase of Φ_∞, corresponding to increasingly southward B_Z IMF. During

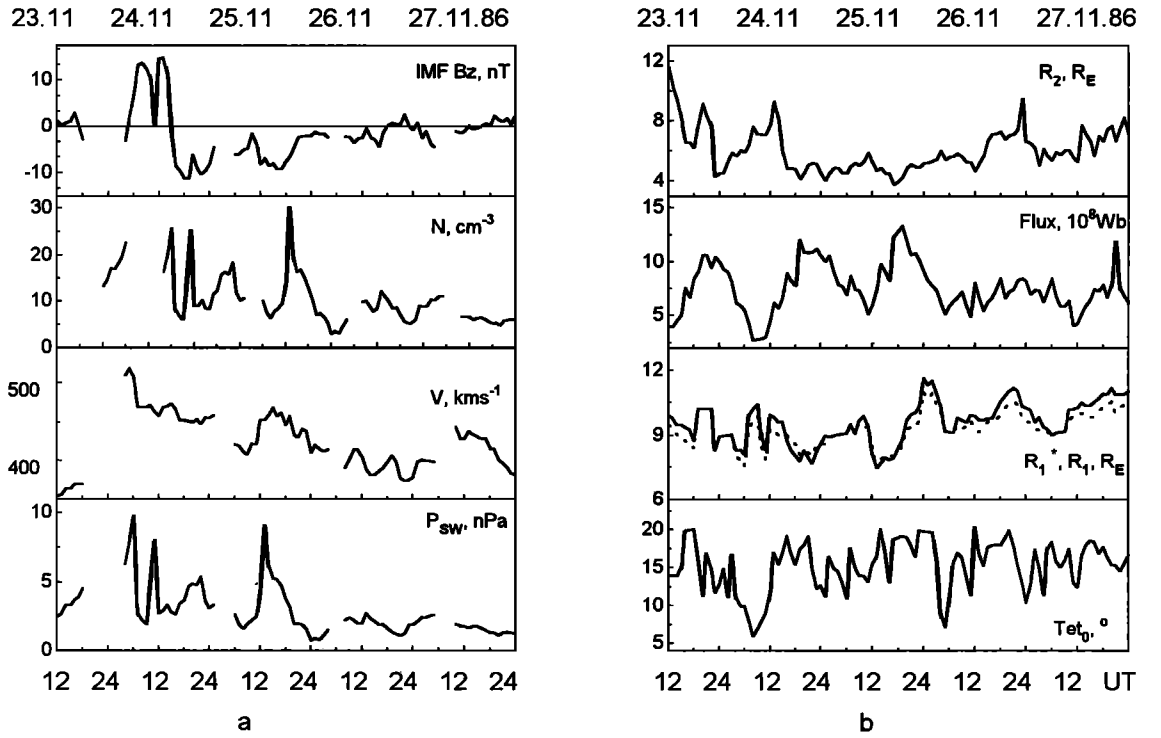

Figure 1. The magnetic storm of November 23-27, 1986. (a) The solar wind data and (b) the paraboloid model input parameters.The solid line shows R_1^*, and the dashed line shows R_1.

the first increase of Φ_∞ the solar wind and IMF data are absent, but it is plausible that $B_Z < 0$. Increases of P_{SW} cause R_1 to decrease. Variations of R_2 do not show any relation to the solar wind parameters, but R_2 decreases when the IMF B_Z turns southward and increases when B_Z turns northward. After 1500 UT on November 24, when B_Z remains < 0 for a long time, R_2 decreases to 4-5 R_E and remains at that level for about ~ 2 days.

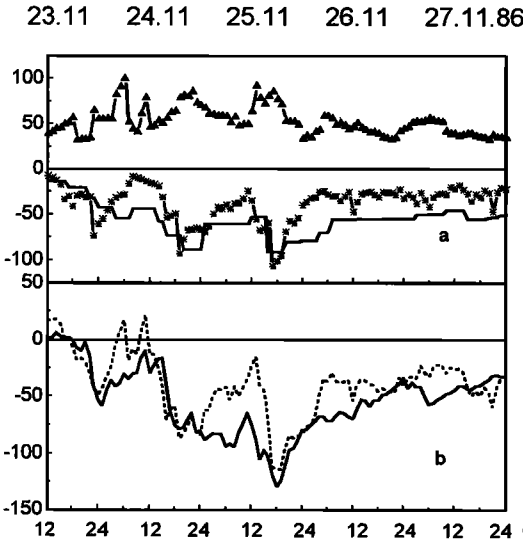

Figure 2. The magnetic storm of November 23-27, 1986. (a) The model tail current (asterisks), the magnetopause screening current (triangles), and the ring current (solid line) contributions to the *Dst* index.(b) A comparison between *Dst* (solid line) and modeled total magnetic field B_M (dashed line).

Figure 2a shows the contributions to *Dst* of the geotail current system B_T, Chapman-Ferraro currents B_{CF}, and the ring current field B_R, including the field of the induced current inside the Earth. There is a full set of solar wind and DMSP satellite data to determine the polar cap radius and midnight auroral oval boundary during this storm. During the period November 23-27, 1986, the AMPTE/CCE satellite crossed the ring current between ~2130 and 0230 LT inbound and between ~1330 and 1830 LT outbound. We used a stepwise linear interpolation between values of B_R calculated from AMPTE/CCE satellite measurements. Fluctuations of B_R are caused by changes in the total ion energy as well as by the MLT asymmetry of the ring current ions. We can not distinguish the MLT dependence of the ring current ions flux and the time variation of the total ion energy by using a single satellite.

As one can see, values of B_{CF}, B_R, and B_T have comparable magnitudes during the main phase of the storm. The time dependence of B_{CF} and B_T is similar, but they have opposite signs. Three B_T extrema during the storm correspond to increases of the polar cap area, which cause magnifications of Φ_∞ and reductions of R_2. Simultaneous increases of B_{CF} are connected to decreases of R_1 and earthward displacement of the magnetopause.

Figure 2b represents a comparison between the model

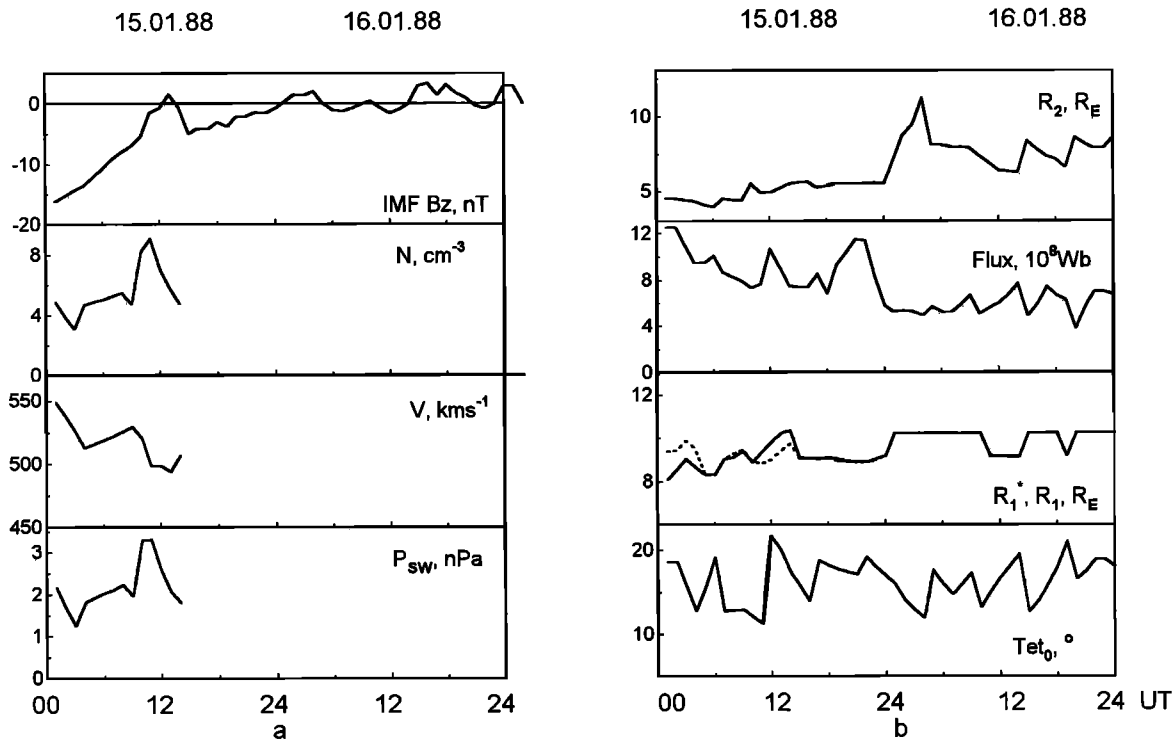

Figure 3. The magnetic storm of January 14-16, 1988. (a) The solar wind data and (b) the paraboloid model input parameters. The solid line shows R_1^*, and the dashed line shows R_1.

magnetic field B_M and the *Dst* index. In general, the comparison shows good agreement between our model and ground-based measurements. However, sometimes the differences reach $\sim$ 25 nT, specifically, from 0000 to 1200 UT on November 25, 1986, and on November 27, 1986, during the recovery phase. Such differences may be caused by the values of R_1 obtained from (6) when the solar wind data are missing. The correlation coefficient r between *Dst* and B_M is 0.82, with standard deviation σ=16.1 nT as calculated for the whole storm interval.

3.2. Magnetic Storm of January 15-16, 1988

The DMSP auroral particle data needed to evaluate the paraboloid model input parameters are available for only 2 days during the storm of January 14-16, 1988. The solar wind plasma data are missing after 1200 UT, January 15, 1988, as well, so R_1 has been calculated using (6). The AMPTE/CCE satellite intersected the ring current inbound near midnight and outbound near 1900 MLT. Figures 3a and 3b show available solar wind data and calculated parameters R_2, Φ_∞, R_1, and θ_0. The auroral particle data used to calculate the tail lobe magnetic flux Φ_∞ and the distance R_2 from the Earth to the tail current sheet's inner edge have been obtained from only one satellite, DMSP F7. Therefore these parameters are calculated with a $\sim$ 1.5-hour time step. We estimated intermediate values of Φ_∞ and R_2 by linear interpolation.

Figure 4a displays the contributions of the ring current B_R, of the magnetopause screening current B_{CF}, and of the tail current B_T to *Dst*. As Figure 4 shows, during the recovery phase of the storm the ring current produces the largest effect on *Dst*. However, at the beginning of the recovery phase the magnetic field produced by the tail current system reaches some tens of

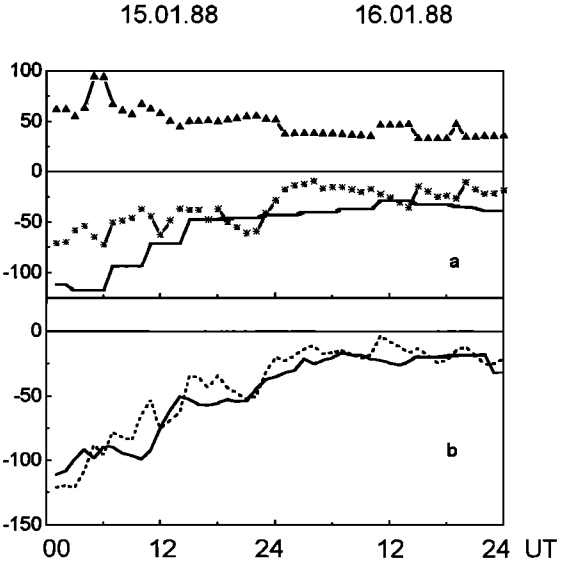

Figure 4. The magnetic storm of January 14-16, 1988. (a) The model tail current (asterisks), the magnetopause screening current (triangles), and the ring current (solid line) contributions to *Dst*. (b) A comparison between *Dst* (solid line) and the model magnetic field B_M (dashed line).

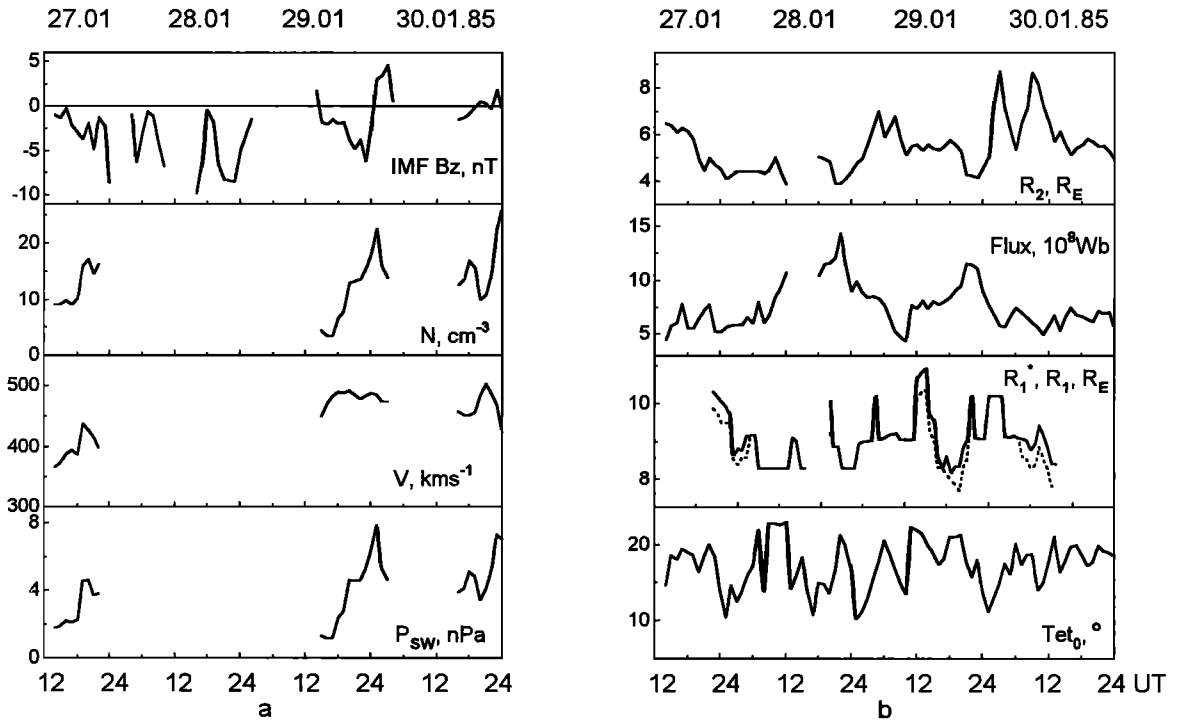

Figure 5. The magnetic storm of January 27-30, 1985. (a) The available solar wind data and (b) the paraboloid model parameters. The solid line shows the parameter R_1^*, and the dashed line shows R_1.

nanotesla. Figure 4b demonstrates a comparison of Dst with the model field B_M during storm recovery, showing that there is good agreement between the two. The correlation coefficient r between B_M and Dst is 0.94, and σ=10.8 nT.

3.3. Magnetic Storm of January 27-30, 1985

Figures 5 and 6 show input data and the model results for the magnetic storm of January 27-30, 1985. There were few solar wind measurements during the storm, and during intervals with no measurements, values of R_1 were calculated using (6). Continuous DMSP F6 and F7 data were available, yielding precipitating plasma boundaries and thus allowing the determination of R_2 and Φ_∞. There are two maxima of Φ_∞. The first of them, near 2200 UT on January 28, is larger, and it occurs near minimum Dst. This location suggests that the increase in $|Dst|$ may be explained by geotail current growth, because the ring current energy determined from AMPTE/CCE data did not increase at this time.

A calculation of the magnetic perturbation due to the ring current based on CCE data taken on January 28, 1985, 1300-1600 UT, gives $B_R = -11$ nT, while earlier, from 0100-0400 UT, CCE data give $B_R = -74$ nT, although Dst shows that the storm grew larger between 0100 and 1400 UT. This indicates that the total ring current ion energy obtained by assuming azimuthal symmetry of the ring current is incorrect. During this storm the AMPTE/CCE satellite crossed L=5 at $\sim$ 0900 MLT inbound and $\sim$ 0300 MLT outbound. We propose that because of local time asymmetry of the ring current, determining the total energy of the ring current ions during the main phase of the storm by using the 0900 MLT data gives values of W and thus of $|B_R|$ that are too small. For this reason the model field B_M was not calculated during the interval 1300-1600 UT.

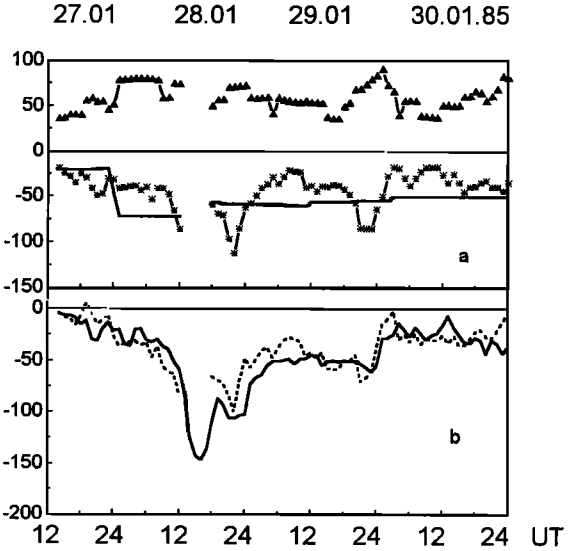

Figure 6. (a) Contributions to Dst of the tail current system (asterisks), of the screening current on the magnetopause (triangles), and of the ring current (solid line); (b) A comparison between the model magnetic field B_M (dashed line) and the Dst index (solid line) during January 27-30, 1985.

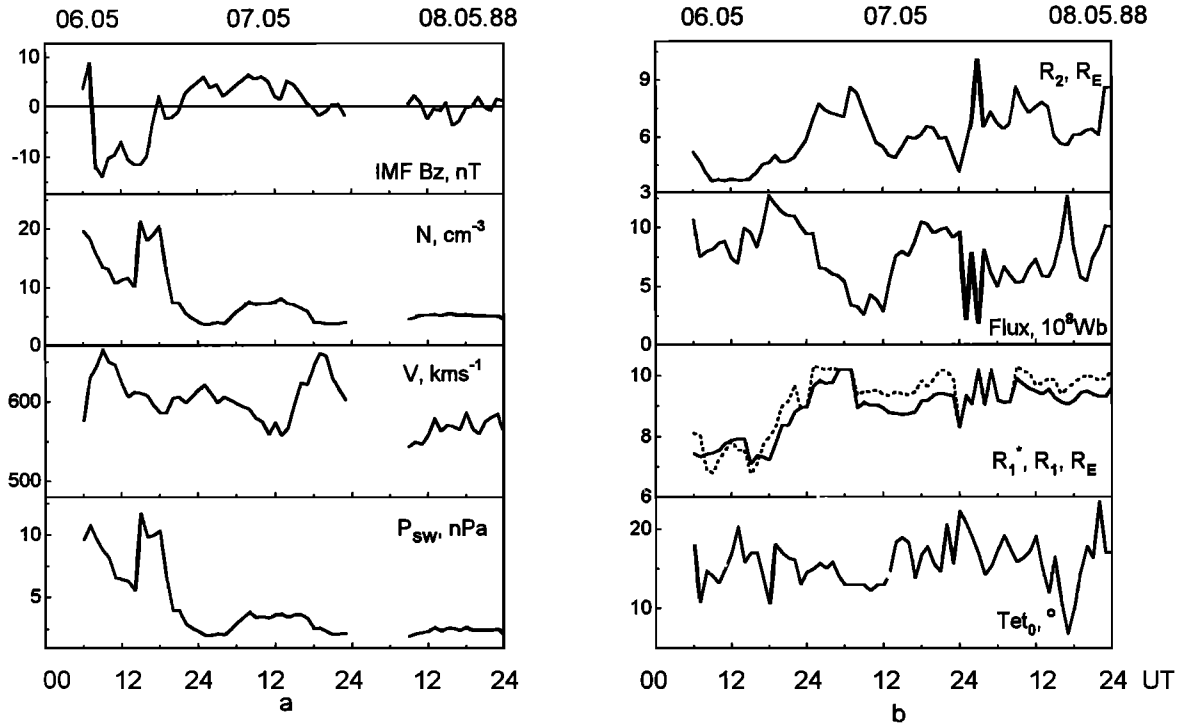

Figure 7. The magnetic storm of May 6-8, 1988. (a) The solar wind data and (b) the paraboloid input parameters. Parameter R_1^* is shown by a solid line, and R_1 is shown by a dashed line.

If the magnetic storm is considered as a whole, then the model field B_M and Dst coincide with accuracy equal to 10-15 nT. Note that the Dst minima at 2200 UT, November 28, and 2200 UT, November 29, coincide with B_T maxima which are the results of abrupt increases of the polar cap area and thus of Φ_∞. The correlation coefficient between Dst and B_M for this storm is equal to 0.79, with $\sigma = 15.5$ nT.

3.4. Magnetic Storm of May 6-8, 1988

Figures 7a and 7b show solar wind data and the values of Φ_∞, R_1, R_2, and θ_0 computed from those observations and used to calculate B_{CF} and B_T during the magnetic storm of May 6-8, 1988. Solar wind data were missing during several short intervals. During the main phase of the storm the IMF B_Z has a large negative value, ~ -10 nT, and the solar wind density N reaches ~ 20 cm^{-3}, producing an increase in P_{SW}, the dynamic plasma pressure. The solar wind velocity V has large values, ~ 600 kms^{-1}, during the whole storm interval. Three maxima in the tail lobe magnetic flux Φ_∞ occur. The first appears connected to the solar wind density or dynamic pressure jump, and the second and third, seemingly, appear connected to a reduction of the geocentric distance R_2. DMSP F8 and F9 satellites' data are available, and they allow us to find the parameters θ_n, θ_{pc}, and R_2 during the whole magnetic storm.

The unsuitable location of AMPTE/CCE on the dayside at 1300-1800 MLT does not allow us to determine the values of B_R correctly. At the time of Dst minimum, 0900-1100 UT, May 6, 1988, the total ring current energy obtained from a satellite pass near 1300 MLT achieves its minimum value, equivalent to $B_R = -59$ nT. Undoubtedly, the small total ring current energy is a consequence of local time asymmetry of the ring current plasma distribution. The asymmetry leads to an underestimate of the total ring current energy when

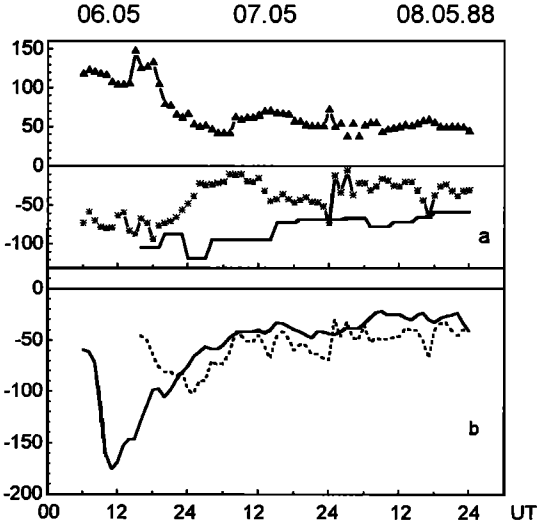

Figure 8. The magnetic storm of May 6-8, 1988. (a) Contributions to Dst due to the tail current (asterisks), the screening magnetopause's current (triangles), and the ring current (solid line). (b) A comparison between model magnetic field B_M (dashed line) and the Dst index (solid line).

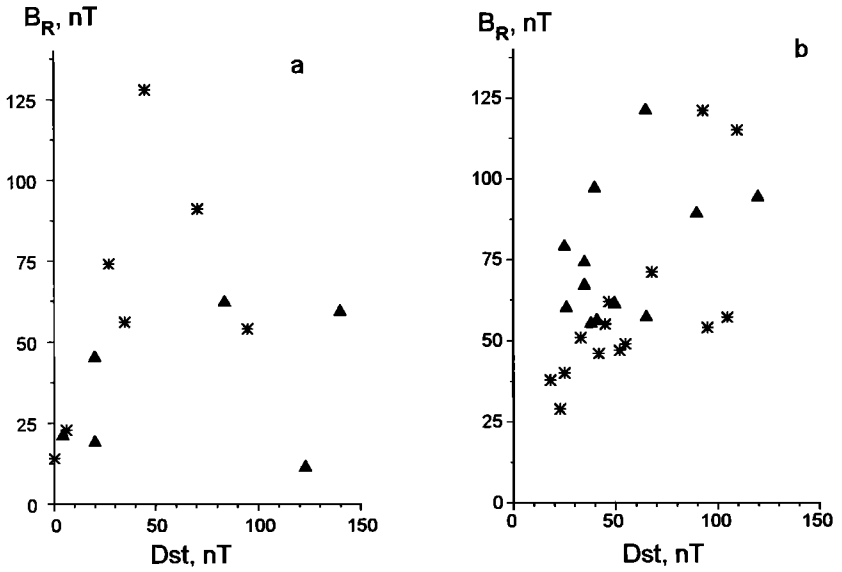

Figure 9. The relation of B_R and Dst: (a) for the main phase of Dst and (b) for the recovery phase of Dst. Asterisks show the nightside, and triangles show the dayside.

CCE measurements are made on the dayside. During the neighboring passes from 0400 to 0700 UT and from 2000 to 2300 UT, when the satellite crossed L=5 at $\sim$ 1800 MLT, B_R is equal to -128 and -89 nT, respectively. For this reason, in Figure 8a we show values for B_R after 1900 UT only.

As in our other cases, Figure 8a shows the magnetic fields B_{CF}, B_T and B_R, comprising the model magnetic disturbance B_M. As is evident from Figure 8a, increases in $|B_T|$ caused by increases of Φ_∞ during the main phase of the storm are compensated for by increases of B_{CF} as a result of small values of $R_1(\sim 7\ R_E)$. During the recovery phase of the storm, B_M is systematically more negative than Dst, but differences do not exceed $\sim$ 20 nT. The correlation coefficient r for this magnetic storm has been calculated two ways: by excluding the time interval 0800-1900 UT, May 6, 1988, r is equal to 0.67 with σ = 15.0 nT; by including all data during the storm, it is equal to 0.60 with σ = 31.9 nT.

In order to define the relationship of the measured total energy of the ring current ions with the MLT of satellite measurements, the dependence of B_R on Dst has been analyzed. In Figure 9 we plot $B_R(Dst)$ for the dayside (0600-1200-1800 MLT) and nightside (1800-0000-0600 MLT), plotting the main phase and the recovery phase separately. Though there is a large dispersion, one can see that B_R increases with $|Dst|$ at all MLT during the recovery phase of storm. The relation is not clear during the main phase if the satellite is on the dayside. Figure 9 shows that measured total ring current energy from satellite passes on the dayside is reduced because of the azimuthal asymmetry of the ring current particles' distribution. An assumption of longitudinal symmetry of the ring current particles is suitable, it seems, for the recovery phase of a storm.

4. Conclusions

We have shown in section 3 that during the main phases of magnetic storms the intensity of the geotail current system magnetic field on the Earth's surface is roughly equal to the intensity of the ring current magnetic field. This result contradicts what is presented in several standard textbooks, according to which the main cause of Dst is the ring current magnetic field.

It is necessary to note that the Dst index is not a pure ring current index [*Campbell*, 1996a]. It should not be considered a simple representation of the ring current in a storm, because other sources contribute to the index's formation. The existence of an important contribution by nightside currents to the symmetric Dst followed from the paper by *Kertz* [1964]. *Campbell* [1973] has described a hypothetical additional contributor to Dst as a triangulated current existing in the midnight magnetosphere at geocentric distances 2-4 R_E.

However, model calculations of perturbations due to these current systems using known values of the current intensities give values of the magnetic field that they produce on the Earth's surface as $\sim 20 - 30$ nT [*Tsyganenko and Sibeck*, 1994]. *Campbell* [1996b], using lognormal distribution functions for the hourly values of the magnetic field amplitude during typical magnetic storms, has concluded that although a ring current certainly exists during a storm, there are many other contributions in the Dst index. However, the relative contributions of different sources to the Dst variation have not been defined.

We have calculated quantitative contributions of different current systems to Dst using the dynamic paraboloid model of the magnetospheric magnetic field. The calculations, carried out using ground-based data and AMPTE/CCE and DMSP satellite measurements,

show that the *Dst* is not an index measuring the ring current only. The other magnetospheric magnetic field sources, particularly the geotail current system and screening currents on the magnetopause, give significant contributions to *Dst*. During the main phase of magnetic storms the contributions of B_T, B_R, and B_{CF} are comparable. However, B_{CF} and B_T effect roughly compensate one another. During the recovery phase the effect of B_R predominates.

Acknowledgments. The authors thank P. T. Newell for DMSP satellite data and A. Grafe and L. I. Gromova for the help in calculations of *Dst*. This work was supported by grant INTAS-RFBR-95-0932 and by the Russian Foundation of Basic Researches project 99-05-65611.

Michel Blanc thanks Tuija I. Pulkkinen and Wallace H. Campbell for their assistance in evaluating this paper.

References

Alexeev, I.I., Regular magnetic field in the Earth's magnetosphere, *Geomagn. Aeron., 18*(4), 656, 1978.

Alexeev, I. I., V. V. Kalegaev, and Y. I. Feldstein, Modelling of magnetic field in the strongly disturbed magnetosphere, *Geomagn. Aeron., 32*(4), 8, 1992.

Alexeev, I. I., E. S. Belenkaya, V. V. Kalegaev, Y. I. Feldstein, and A. Grafe, Magnetic storms and magnetotail currents, *J. Geophys. Res., 101*, 7737, 1996.

Arykov, A. A., and Y. P. Maltsev, Contribution of various sources to the geomagnetic storm field, *Geomagn. Aeron., 33*(6), 67, 1993.

Campbell, W. H., The field levels near midnight at low and equatorial geomagnetic stations, *J. Atmos. Terr. Phys., 35*, 1127, 1973.

Campbell, W. H., *Dst* is not a pure ring current index, *Eos Trans. AGU, 77*(30), 283, 1996a.

Campbell, W. H., Geomagnetic storms, the *Dst* ring-current myth and lognormal distributions, *J. Atmos. Terr. Phys., 58*, 1171, 1996b.

Dremukhina, L. A., P. Ivanova, and Y. I. Feldstein, Development of the ring current and its modelling at the Panaguriste Observatory, *Geomagn. Aeron., 30*(5), 862, 1990.

Feldstein, Y. I., and Y. I. Galperin, Structure of the auroral precipitations in the nightside sector of the magnetosphere, *Cosmic Res., Engl. Transl., 34*, 227, 1996.

Feldstein, Y. I., and G. V. Starkov, Dynamics of auroral belt and polar geomagnetic disturbances, *Planet. Space Sci., 15*, 209, 1967.

Fok, M.-C., J. U. Kozyra, A. F. Nagy, C. E. Rasmussen, and G. V. Khazanov, Decay of equatorial ring current ions and associated aeronomical consequences, *J. Geophys. Res., 98*, 381, 1993.

Kalegaev, V. V., I. I. Alexeev, Y. I. Feldstein, L. I. Gromova, A. Grafe, and M. Greenspan, Magnetic flux in the magnetotail lobes and *Dst* dynamics during magnetic storms, *Geomagn. Aeron., 38*(3), 10, 1998.

Kertz, W., Ring current variations during the IGY, *Ann. Int. Geophys. Year, 35*, 49, 1964.

Kistler, I. M., F. M. Ipavich, D. C. Hamilton, G. Gloecker, B. Wilken, G. Kremser, and W. Studemann, Energy spectra of the major ion species in the ring current during geomagnetic storms, *J. Geophys. Res., 94*, 3579, 1989.

Kozyra, J. U., Sources and losses of ring current ions: An update, *Adv. Space Res., 9*, 171, 1989.

Maltsev, Y. P., Relation of Dst-variation to magnetospheric geometry, *Geomagn. Aeron., 31*(3), 567, 1991.

Maltsev, Y. P., A. A. Arykov, E. G. Belova, B. B. Gvozdevsky, and V. V. Safargaleev, Magnetic flux technique for calculating storm-time depression, Paper presented at International Conference on Magnetic Storms, Sol. Terr. Environ. Lab., Nagoya Univ., Rikubetsu, Hokkaido, Japan, Oct. 6-8, 1994.

Mead, G. D. Deformation of the geomagnetic field by the solar wind, *J. Geophys. Res., 69*, 1181, 1964.

Newell, P. T., Y. I. Feldstein, Y. I. Galperin, and C.-I. Meng, The morphology of nightside precipitation, *J. Geophys. Res., 101*, 10,737, 1996.

Roelof, E. C., and D. G. Sibeck, 'The magnetopause shape as a bivariate function of IMF Bz and solar wind dynamic pressure, *J. Geophys. Res., 98*, 21,421, 1993.

Shue, J.-H., J. K. Chao, H. C. Fu, C. T. Russell, P. Song, K. K. Khurana, and H. J. Singer, A new functional form to study the solar wind control of the magnetopause size and shape, *J. Geophys. Res., 102*, 9497, 1997.

Sun, W., B.-H. Ahn, S.-I. Akasofu, and Y. Kamide, A comparison of the observed mid-latitude magnetic disturbance fields with those reproduced from the high-latitude modeling current system, *J. Geophys. Res., 89*, 10,881, 1984.

Takahashi, S., M. Takeda, and Y. Yamada, Simulation of storm-time partial ring current system and the dawn-dusk asymmetry of geomagnetic variation, *Planet. Space Sci., 39*, 821, 1991.

Tsyganenko, N. A., and D. G. Sibeck, Concerning flux erosion from the dayside magnetosphere, *J. Geophys. Res., 99*, 13,425, 1994.

I. I. Alexeev and V. V. Kalegaev, Institute of Nuclear Physics, Moscow State University, 119899 Moscow, Russia.

L. A. Dremukhina and Y. I. Feldstein, IZMIRAN, 142092 Troitsk, Moscow Region, Russia.

M. E. Greenspan, Department of Physics, University of Maryland, College Park, MD 20742.

(Received October 21, 1998; revised May 25, 1999; accepted June 7, 1999.)